

Structural evolution during annealing of laser-ablation-deposited Ge-Sn-Se amorphous films

Didarul Islam* and R. L. Cappelletti

*Department of Physics and Astronomy, Condensed Matter and Surface Sciences Program,
Ohio University, Athens, Ohio 45701*

(Received 30 November 1990)

Optical transmittance measurements on virgin and annealed laser-ablated amorphous Ge-Sn-Se films are presented. The film compositions were near those of the pseudobinary source glasses: $(\text{GeSe}_2)_{1-x}(\text{SnSe}_2)_x$. Results are analyzed for the energy, annealing temperature, and composition dependences of the optical constants. The Tauc energy gap and the Urbach tail width extracted from the absorption coefficient are found to vary nonmonotonically with composition in the annealed films, in agreement with measurements of other quantities on bulk glasses in this system. This behavior is discussed in terms of homopolar-bond defects in the glass structure whose concentration evolves with annealing towards intrinsic values deriving from mechanical constraints in the relaxed glasses.

I. INTRODUCTION

The structure of multicomponent stoichiometric network glasses is of continuing interest, particularly in the chalcogenide glasses. Are the atoms arranged in a chemically ordered covalent random network (COCRN), or do other molecular fragments enter the structure? What role does chemical ordering play in determining the structure as compared to the influence of mechanical forces such as strain associated with bond distortions?

One system in which such questions have been addressed is the pseudobinary glass $g-(\text{GeSe}_2)_{1-x}(\text{SnSe}_2)_x$. Naively one expects GeSe_2 to be an example of a COCRN of corner and edge sharing tetrahedra, and the pseudobinary to follow suit, at least over some composition range. On the other hand, according to constraint-counting arguments GeSe_2 is an "overconstrained" glass in which chemical order may be broken by "mechanical" forces resulting in the appearance of fragments departing from the $\text{Ge}(\text{Se}_{1/2})_4$ tetrahedron characterized by an intrinsic concentration of homopolar bonds.

Bond-stretching forces acting as mechanical constraints are present in Ge, Se, and Sn. Bond-bending constraints are important in Ge and Se but may be ignored in Sn because the corresponding spring constant is weak compared to Ge and Se. It is this fact which makes $(\text{GeSe}_2)_{1-x}(\text{SnSe}_2)_x$ such a useful glass system to study. The addition of Sn is expected to reduce the role of mechanical forces in determining structure because it reduces the number of constraints per atom and allows one to tune the system from overconstrained to underconstrained regimes.

A considerable body of research addressing the issue of structure in bulk glasses in this system indicates that there is nonmonotonic behavior with increasing Sn concentration in several measured quantities.¹⁻³ The purpose of this study is to attempt to produce a highly disturbed amorphous form of this material which might be expected to exhibit monotonic behavior with alloying because it is more "random" than the glassy form, and then

to relax it toward the glassy form while watching for the emergence of nonmonotonic behavior.

In particular, we chose to produce amorphous films by laser-ablation-deposition and to measure optical transmittance for several concentrations as a function of annealing. Optical transmittance yields quantities which are measures of internal disorder and has the advantage of being convenient and simple to perform. Moreover, as we shall see, the results of these measurements are in agreement with previous studies in exhibiting nonmonotonic behavior with alloying and hence support the picture of qualitative structural evolution with alloying in this system.

In Secs. II and III of this paper we present details of sample preparation, film composition, and the optical measurements. In Sec. IV we describe the results of the optical measurements and quantities obtained from them. The behavior of these quantities and their interpretation is discussed in Sec. V, and the conclusions emerging from this work are summarized in Sec. VI.

II. EXPERIMENTAL DETAILS

Bulk $(\text{GeSe}_2)_{1-x}(\text{SnSe}_2)_x$ glasses were prepared by melt-quenching elemental components in chemically cleaned quartz tubes. The tubes were evacuated to $\sim 10^{-6}$ Torr before sealing. Tin (A. D. Mackay, Inc., N.Y.) and selenium (Johnson Mathey, Inc., Seabrook, N.H.), both of 99.999% purity, and germanium (Johnson Mathey) of 99.9999% purity were used. The tubes were heated to 950°C in a vertical position for approximately two days and inverted intermittently to ensure thorough mixing. They were then rapidly quenched in cold water resulting in the glassy phase of the material. These source glasses were used as targets for laser ablation.

The films were deposited onto chemically cleaned Corning 2948 microscope slides. The deposition was done by ablating the targets using a LUMONICS TE-860-2 krypton-fluoride excimer laser. The films were prepared under a vacuum of $\sim 10^{-5}$ Torr. The sample

preparation procedure is described in detail in Ref. 4. Films of thicknesses $\sim 2.0 \mu\text{m}$ were prepared for source glass compositions $(\text{GeSe}_2)_{1-x}(\text{SnSe}_2)_x$ with x ranging from 0 to 0.25.

Optical absorption measurements were made on a Perkin-Elmer LAMBDA-9 Spectrophotometer in the dual-beam mode with a blank substrate in the reference slot. The data collection procedure was designed to optimize the accuracy of the analysis. The latter uses a method described in Ref. 5 and is based on a procedure proposed by Swanepoel.⁶ The data collection for each film, after annealing at a given temperature, was carried out in five steps. Two slow scans were made, the first between 3000 nm and 1200 nm and the second between 860 nm and 550 nm, both in the transmittance mode. The locations of the extrema were thus identified. In the next step the transmittance at each of these extrema was determined with greater precision. This was achieved by taking repeated transmittance measurements at the same wavelength to obtain the mean value. A slow scan was also made in the absorbance mode between 600 nm and 450 nm. This last scan and the transmittance at the extrema were the actual data that were finally analyzed to obtain the thickness and the optical constants of each film.

The samples were annealed in an atmosphere of argon of 99.999% purity, introducing the gas through a liquid nitrogen cold trap to reduce residual moisture. The annealing temperatures selected were 370, 440, and 510 K. The duration of annealing at each temperature was 20 h. Each sample was brought back to room temperature for transmittance data collection before the next annealing stage. Annealing beyond 510 K was attempted for a few samples. In every case it was noticed that yellow patches appeared on the films and the smooth surface texture was destroyed. Consequently optical absorption measurements were limited to samples annealed at 510 K and below.

III. FILM COMPOSITIONS

In preparing thin films of alloy glasses from a bulk source two major complications arise. First, the vapor pressure of each component is different. Second, the film composition is also affected by the differences in the sticking coefficients of each atomic species. The first difficulty was overcome by employing the laser-ablation technique in which the ablated plume has a composition closer to that of the target than would a thermal vapor.

We did not make an attempt to overcome the second difficulty although in principle it could be done by suitably adjusting the composition of the source bulk glass to compensate for the differences in the sticking coefficients of the components.

The compositions of the films were determined using proton-induced x-ray emission (PIXE) the details of which are discussed in Ref. 4. The uncertainties of the measurements are estimated to be $\sim 2\%$. In referring to the different films in subsequent discussions in this paper reference will be made to the tin content x of the corresponding source glasses, but in the actual films the Ge and Sn portions did not sum to one in general. The compositions of the source glasses and of deposited films are given in Table I along with $\langle r_{\text{eff}} \rangle$ defined below.

IV. RESULTS

In describing our results comparisons are made with other work on similar glasses. Glassy networks are influenced by mechanical constraints associated with the atomic bonding. Although compositions may vary the number of constraints per atom, N_c , can be used as a common parameter to describe a variety of network glasses. We describe our results by defining an average effective coordination number $\langle r_{\text{eff}} \rangle$, a parameter related to N_c as explained below.

In a covalently bonded glass network like $\text{Ge}_x\text{Se}_{1-x}$ two types of constraints, bond-bending and bond-stretching, need to be counted.⁷ For an atomic species with coordination number r the number of constraints per atom arising from bond-bending is $N_c = 2r - 3$ and from bond-stretching is $N_c = r/2$. Mössbauer experiments⁸ show that in $(\text{GeSe}_2)_{1-x}(\text{SnSe}_2)_x$ pseudobinary alloy glasses Sn replaces Ge in the network. The weaker bond-bending forces in Sn allow one to ignore the associated constraints. The addition of Sn thus reduces the number of constraints per atom and allows one to tune the system through the rigidity-percolation threshold which theory predicts to be at $\langle r_{\text{eff}} \rangle = 2.4$.⁷

Table II shows the values and expressions for the average number of constraints per atom and the average coordination number for different compositions of this class of glasses. For $\text{Ge}_x\text{Se}_{1-x}$, the average coordination number per atom is $\langle r \rangle = (\frac{2}{5})(N_c + 3)$. This formula can be used to define and calculate an effective average coordination number $\langle r_{\text{eff}} \rangle$ as shown in Table II. Thus $\langle r_{\text{eff}} \rangle$ is a common parameter to compare the results obtained for

TABLE I. Source glass and deposited film compositions and $\langle r_{\text{eff}} \rangle$ for the films studied.

Source glass			Deposited film			
Ge	Sn	Se	Ge	Sn	Se	$\langle r_{\text{eff}} \rangle$
1	0	2	0.982	0	2	2.66
0.95	0.05	2	0.858	0.051	2	2.59
0.90	0.10	2	0.801	0.109	2	2.55
0.85	0.15	2	0.809	0.168	2	2.54
0.80	0.20	2	0.754	0.235	2	2.50
0.75	0.25	2	0.579	0.271	2	2.41

TABLE II. Values and expressions for the number of constraints per atom N_c and the average coordination number $\langle r \rangle$ for ternary and pseudobinary glasses in the $\text{Ge}_{1-x}\text{Se}_x$ class. For $\text{Ge}_x\text{Se}_{1-x}$, $\langle r \rangle = 2(N_c + 3)/5$. We may define $\langle r_{\text{eff}} \rangle$ for the other glasses using this formula inserting the appropriate N_c in each case.

Glass type	N_c	$\langle r \rangle$
GeSe_2	$\frac{11}{3}$	$\frac{8}{3}$
$\text{Ge}_{1-x}\text{Sn}_x\text{Se}_2$	$(11 - 5x)/3$	$\frac{8}{3}$
$\text{Ge}_y\text{Sn}_x\text{Se}_2$	$(2x + 7y + 4)/(x + y + 2)$	$4(x + y + 1)/(x + y + 2)$
$\text{Ge}_x\text{Se}_{1-x}$	$5x + 2$	$2x + 2$

glasses having a variety of compositions with reference to the well-studied variable constraint glass $\text{Ge}_x\text{Se}_{1-x}$.⁹⁻¹²

The thickness and the refractive index of each film were determined with 2% precision from transmittance extrema data between 3000 and 1200 nm. Assuming a Cauchy-type of behavior the $n(\lambda)$ were extrapolated to shorter wavelengths. Within the experimental uncertainties the thickness and refractive index did not change with annealing.

The refractive indices $n(\lambda)$ of films of different tin content are shown in Fig. 1. The general trend is that n increases as $\langle r_{\text{eff}} \rangle$ decreases with a sharp step evident around $\langle r_{\text{eff}} \rangle = 2.55$. These results agree well, both in magnitudes and general trends, with independent results obtained for bulk glasses of the same system by ellipsometry in another laboratory¹³ as seen in Fig. 2.

Two parameters bearing signatures of structural changes within the glass network are the inverse slope (or width) σ of the Urbach tail [the linear portion of the curve in a $\ln\alpha(E)$ versus E plot, see Fig. 4, for example] and the optical gap. The absorption edge lies in the range between 860 and 450 nm. A set of raw transmittance data in this region for an $x = 0.20$ sample is shown in Fig. 3. As the annealing proceeds the absorption edge shifts toward higher energies. This is typical of all films

investigated.

Figure 4 shows the shift of the absorption coefficient, $\alpha(E)$, of an $x = 0.20$ film on annealing it for 20 h at 510 K. Moreover, the Urbach tail width, σ , has an overall tendency to decrease on annealing. This effect is most dramatic for $x = 0.20$ shown in Fig. 5 which is a plot of σ versus annealing temperature for four different samples of $x = 0.20$. Sample 1 was annealed successively at different temperatures as discussed earlier. Sample 2 was annealed for 20 h only at 440 K and sample 3 only at 510 K. The results in this figure are for films from a single deposition, but the films are of different thicknesses. They show that at each of the two annealing temperatures 440 and 510 K sample 1 has a lower σ compared to samples 2 and 3 indicating that it is more annealed. This is expected since sample 1 has gone through the annealing process over longer periods. Only the as-deposited result is shown for sample 4. It was annealed at 560 K but this process introduced yellow spots and surface roughness, as described earlier, rendering transmission data useless.

Figure 6 shows σ plotted against $\langle r_{\text{eff}} \rangle$ for both virgin and annealed films. Apart from the general trend of σ decreasing somewhat with annealing, the most remarkable feature here is the sharp decrease at $\langle r_{\text{eff}} \rangle = 2.5$ which clearly renders the behavior of annealed σ non-monotonic in $\langle r_{\text{eff}} \rangle$. As will be discussed below this

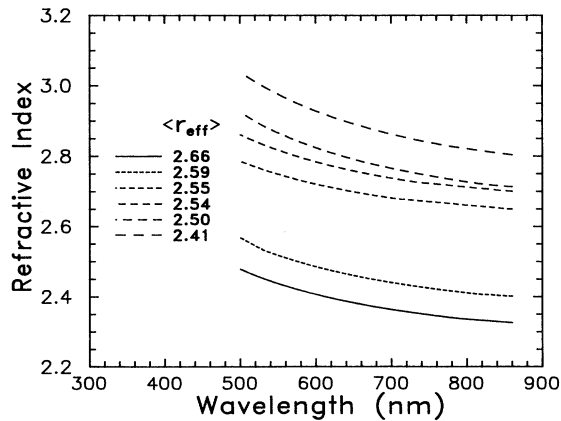


FIG. 1. Refractive index for films of $\text{Ge}_{1-x}\text{Sn}_x\text{Se}_2$ vs wavelength.

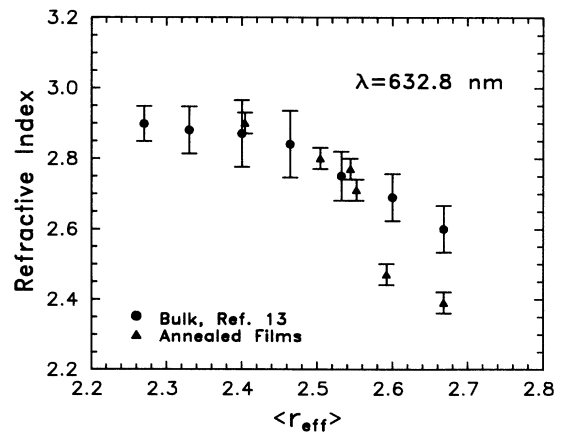


FIG. 2. Refractive index at $\lambda = 632.8 \text{ nm}$ for $\text{Ge}_{1-x}\text{Sn}_x\text{Se}_2$. The results for bulk glasses were independently obtained by ellipsometry (Ref. 13).

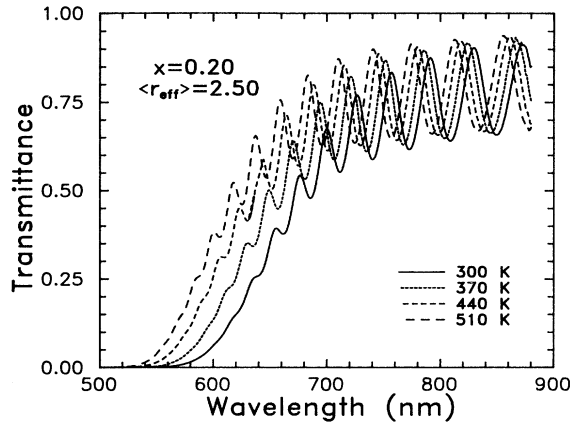


FIG. 3. Transmittance data for an $x=0.20$ film.

feature departs from current ideas relating the Urbach tail parameter to the glass transition temperature T_g which is a monotonic function of $\langle r_{\text{eff}} \rangle$ in this region.¹

For the optical gap we use the Tauc gap, E_g^{opt} , obtained by fitting data to the formula $(\alpha E)^{1/2} \propto (E - E_g^{\text{opt}})$.¹⁴ Figure 7 shows the absorption coefficient data for a $x=0.2$ ($\langle r_{\text{eff}} \rangle=2.5$) sample plotted to determine E_g^{opt} . For the $(\text{GeSe}_2)_{1-x}(\text{SnSe}_2)_x$ glassy films the optical gap generally increases on annealing. The increments appear to slow down around an annealing temperature of 510 K as seen in Fig. 8.

A plot of the $\langle r_{\text{eff}} \rangle$ dependence of annealed E_g^{opt} from this work and E_0 for bulk samples from the work of Mikrut and McNeil³ is shown in Fig. 9. Both the annealed films and bulk samples show a departure from monotonic behavior in the form of a broad peak near $\langle r_{\text{eff}} \rangle=2.5$ superimposed on a linear background. (Subtraction of the background would shift the peak to a lower value of $\langle r_{\text{eff}} \rangle$.)

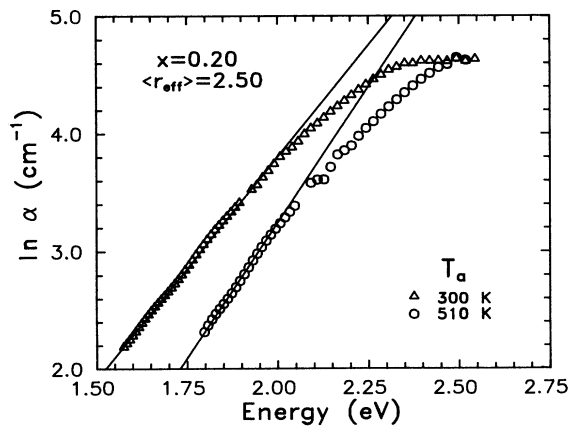


FIG. 4. Absorption coefficient vs photon energy for an $x=0.20$ sample at two annealing temperatures showing the shift of the absorption edge and of the Urbach tail slope.

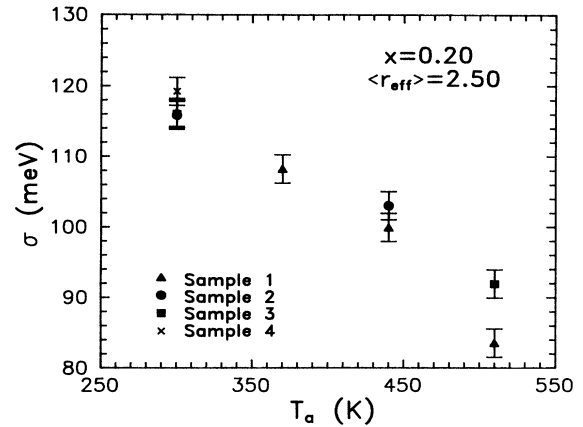


FIG. 5. Inverse Urbach tail slope, σ , vs annealing temperature for four samples at $x=0.20$.

V. DISCUSSION

We discuss the energy gap first. The “energy gap” E_0 of Ref. 3 is actually the value of the photon energy at which $\alpha=150 \text{ cm}^{-1}$. Generally this estimate of the gap energy is lower than the Tauc gap, E_g^{opt} which we use. Thus the agreement between the results for these annealed films and the bulk glasses or Ref. 3 suggests that the annealed films are approaching bulk glasses in their properties.

This suggestion is further supported by the work of Wells *et al.*¹⁵ who use a Sn Mössbauer probe to measure the degree of chemical order in evaporated and annealed films of a Ge-Sn-Se glass. They find Sn in two sites, one with heteropolar bonding and one with homopolar bonding. [If the structure were a perfect COCRN of Ge (or Sn) $(\text{Sn}_{1/2})_4$ tetrahedra the homopolar-bonded Sn would be absent.] The fraction of heteropolar-bonded Sn in their annealed film approaches that of the bulk glass of the same composition.

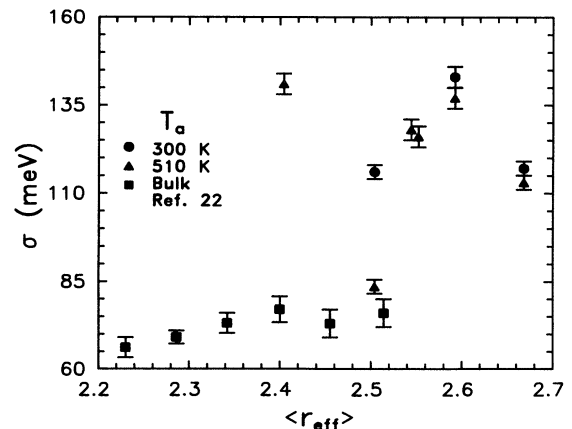


FIG. 6. σ vs $\langle r_{\text{eff}} \rangle$ for films of this work and bulk samples from Ref. 22.

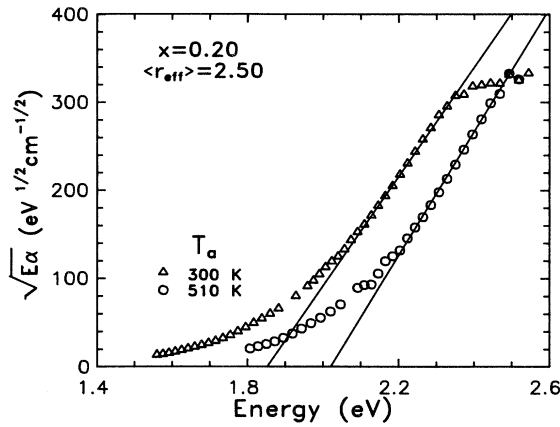


FIG. 7. Absorption coefficient for $x=0.20$ plotted to extract the Tauc gap. E_g^{opt} is obtained as the energy intercept of a fit to the linear region.

The appearance of nonmonotonic behavior in the energy gap as a function of $\langle r_{\text{eff}} \rangle$ is reminiscent of the results seen in other studies.^{2,3} Most prominently, Stevens *et al.*¹ observed the Mössbauer heteropolar-bonded Sn fraction and the Raman A_1 companion mode amplitude to oscillate as a function of Sn concentration in bulk $(\text{GeSe}_2)_{1-x}(\text{SnSe}_2)_x$ glasses in a range over which the glass transition temperature varies monotonically. Their results are reproduced in Fig. 10(a). In particular, the fraction of heteropolar-bonded Sn goes to 1 at $x=0.35$ ($\langle r_{\text{eff}} \rangle = 2.433$) near the rigidity percolation threshold of $\langle r_{\text{eff}} \rangle = 2.4$. They construe this as evidence that only at this special composition is the glass organized in a COCRN. This remarkable result means that at this concentration chemical attraction overwhelms the free energy reduction which could accompany bond strain relaxation and that could accompany the increased entropy associated with “wrong” bonds.

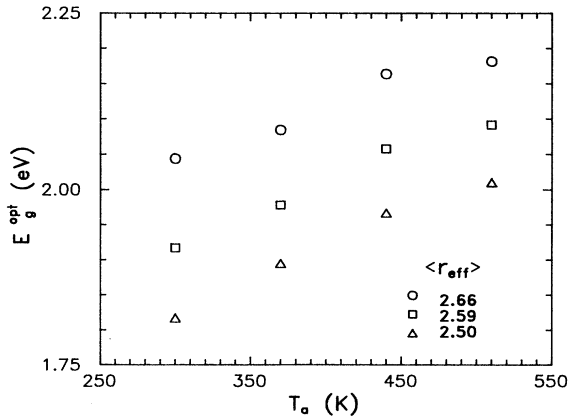


FIG. 8. Energy gap vs annealing temperature for three samples.

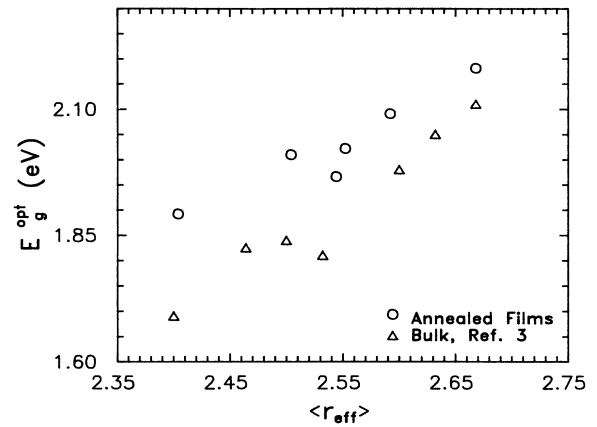


FIG. 9. Energy gap vs $\langle r_{\text{eff}} \rangle$ for the annealed films of this work and bulk samples of Ref. 3.

For lower Sn concentrations (including GeSe_2), where the number of constraints per atom exceeds the number of degrees of freedom, 3, the heteropolar-bonded Sn concentration is found to be less than one. Stevens *et al.* conclude that the appearance of intrinsic homopolar bond defects occurs as the system attempts to relieve the extra strain energy associated with overconstraint. Thus the nonmonotonic behavior of various properties observed in these glasses is explained in terms of an inter-

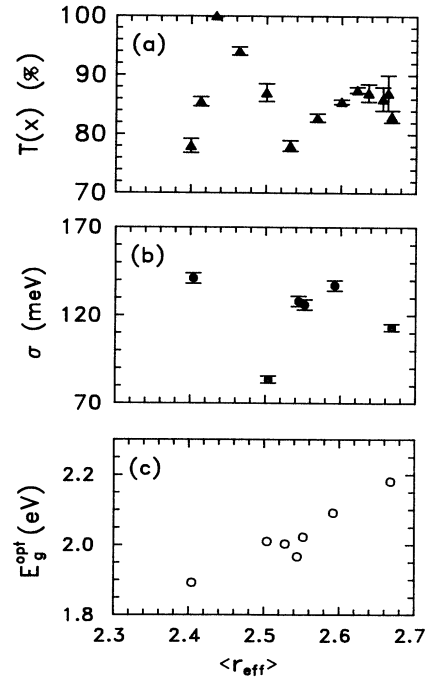


FIG. 10. (a) The fraction of Sn atoms exhibiting heteropolar bonding T from Ref. 1. (b) The energy gap E_g^{opt} and (c) σ vs $\langle r_{\text{eff}} \rangle$ plotted together to exhibit correlations.

play between “mechanical” and “chemical” forces which affect the structure of the glasses as a function of $\langle r_{\text{eff}} \rangle$.

Applying these findings to our results, we recall that the Tauc gap is determined by the conduction and valence band edges and is not very sensitive to the band tails. We expect that the presence of homopolar bond defects will broaden valence and conduction band edges. One could thus get a peak in E_g^{opt} near $\langle r_{\text{eff}} \rangle = 2.43$ in annealed glasses where these defects disappear and the band edges sharpen up. Moreover, the fraction of homopolar bonded Sn decreases with annealing,¹⁶ which would be consistent with an increase of the gap width with annealing as observed in this experiment.

Next we discuss the Urbach parameter, σ . The significance of this parameter is discussed by several authors,^{17–20} most recently by Chan *et al.*²¹ It has been identified with local fluctuations of electronic potential energies arising from the randomness mainly frozen into the network as the glass is formed. It therefore is most sensitive to structural disorder affecting the shape of electronic band tails.

In terms of the “mechanical” and “chemical” forces discussed earlier one expects both homopolar bond defects and strains having a wide energy distribution to be frozen into these films deposited on a room temperature substrate from a laser-ablated plume. Thus the as-deposited values of σ reflect the large amount of frozen-in disorder. This disorder, of course, cannot be characterized simply by the glass temperature T_g since it is captured in quite a different way incorporating energies well beyond the thermal distribution at T_g . This may account for the fact that the size of σ in the as-deposited films is larger than that seen in similar bulk glasses by Ksendov *et al.*²² which have been produced via quenching from the melt. The results of Ref. 22 for $\text{Ge}_{1-x}\text{Sn}_x\text{Se}_{2.5}$ are shown for comparison in Fig. 6 as solid squares. As discussed in Ref. 21 σ is proportional to the T_g in such a case.

Moreover, as our films relax upon annealing toward bulk glass behavior the disorder which relaxes away does not necessarily reduce to that characteristic of the bulk glass since high energy disturbances incorporated during laser ablation deposition might require more thermal energy and a longer annealing time than was available in our protocol. This may explain why, with an important exception to be discussed, σ in our annealed films remains higher than was observed in Ref. 22.

The exception is the datum at $\langle r_{\text{eff}} \rangle = 2.5$. All samples measured at this concentration showed the same behavior with annealing. The point plotted is for the sample following the same annealing protocol as the samples at the other $\langle r_{\text{eff}} \rangle$ values. As yet we have no explanation for

the enhanced annealing effect at this value of $\langle r_{\text{eff}} \rangle$.

It is interesting to note in Fig. 10 that there is an apparent anticorrelation in the behavior of E_g^{opt} and σ as functions of $\langle r_{\text{eff}} \rangle$. Such an anticorrelation has been found to hold quantitatively in hydrogenated amorphous silicon.²⁰ In Ref. 20 the anticorrelation is explained in terms of the opposing effects which disorder (both thermal and structural) has on these two parameters.

It is revealing to plot σ and the heteropolar-bonded Sn fraction T from Ref. 1 versus $\langle r_{\text{eff}} \rangle$ together in Fig. 10. We see that there is strong correlation in the behavior of these two quantities. In fact the minimum in σ occurs very near the minimum in T , i.e., where the homopolar bond defects are a maximum. In Ref. 1 this minimum in T is interpreted in terms of the onset of reorganization of the network into a continuous random network. Thus the two salient facts for any future explanation are that the value of σ at the minimum is nearly the same as for a bulk glass, indicating an enhanced relaxation with annealing from the as-deposited state compared to other $\langle r_{\text{eff}} \rangle$ values, and that the behavior of σ in these annealed laser-ablated films closely follows the heteropolar-bonded Sn fraction in bulk glasses.

VI. CONCLUSIONS

We have prepared thin films of Ge-Sn-Se glasses by laser-ablation deposition and measured their optical transmittances as a function of annealing. Values of the Tauc gap, E_g^{opt} , and the inverse slope of the Urbach tail, σ , were obtained from these measurements. The as-deposited films appear to be characterized by the presence of significant amounts of frozen-in defects which cause enhancement of σ and the depression of E_g^{opt} . As the films are annealed they approach the behavior of bulk glasses, exhibiting a nonmonotonic behavior in the measured quantities vs $\langle r_{\text{eff}} \rangle$. This nonmonotonic behavior is consistent with other measurements on bulk glasses in this pseudobinary alloy which have revealed the presence of concentration-dependent intrinsic homopolar-bond defects when the number of mechanical constraints exceeds the number of degrees of freedom.

ACKNOWLEDGMENTS

This work has been supported in part by an Academic Challenge Grant from the State of Ohio Board of Regents. Thanks are due to the Ohio University Department of Chemistry for the use of laser and spectrophotometer facilities. R.L.C. wishes to express thanks to the Reactor Radiation Division of NIST for its hospitality during a sabbatical leave in which this paper was written.

*Current address: Department of Physics, Central Michigan University, Mount Pleasant, MI 48859.

¹M. Stevens, P. Boolchand, and J. G. Hernandez, *Phys. Rev. B* **31**, 981 (1985).

²C. F. Niederriter and R. L. Cappelletti, *Solid State Commun.*

61, 527 (1987).

³J. M. Mikrut and L. E. McNeil, *J. Non-Cryst. Solids* **114**, 127 (1989).

⁴D. Islam, C. E. Brient, and R. L. Cappelletti, *J. Mater. Res.* **5**, 511 (1990).

- ⁵Didarul Islam, Ph.D. thesis, Ohio University, 1989.
- ⁶R. Swanepoel, *J. Phys. E* **16**, 1214 (1983).
- ⁷J. C. Phillips, *J. Non-Cryst. Solids* **34**, 153 (1979); **43**, 37 (1981); **47**, 203 (1983); also see G. H. Dohler, R. Dandolofo and H. Bilz, *ibid.* **42**, 87 (1980); J. C. Phillips and M. F. Thorpe, *Solid State Commun.* **53**, 699 (1985).
- ⁸P. Boolchand and M. Stevens, *Phys. Rev. B* **29**, 1 (1984).
- ⁹P. Boolchand, R. N. Enzweiler, R. L. Cappelletti, W. A. Kamitakahara, Y. Cai, and M. F. Thorpe, *Solid State Ionics* **39**, 81 (1990); W. A. Kamitakahara, R. L. Cappelletti, P. Boolchand, B. Halfpap, F. Gampf, D. A. Neumann, and H. Mutka, *Phys. Rev. B* **44**, 94 (1991).
- ¹⁰S. S. Yun, Hui Li, R. L. Cappelletti, R. N. Enzweiler, and P. Boolchand, *Phys. Rev. B* **39**, 8702 (1989).
- ¹¹Y. Ito, S. Kashida, and K. Murase, *Solid State Commun.* **65**, 449 (1988).
- ¹²Y. Cai and M. F. Thorpe, *Phys. Rev. B* **40**, 10535 (1989).
- ¹³L. W. Martin, L. E. McNeil, and J. M. Mikrut, *Philos. Mag. B* **61**, 957 (1990).
- ¹⁴J. Tauc, *Mat. Res. Bull.* **5**, 721 (1970).
- ¹⁵J. Wells, P. Boolchand, Didarul Islam, and R. L. Cappelletti (unpublished).
- ¹⁶P. Boolchand, R. N. Enzweiler, and M. Tenhover, *Diffusion Defect Data* **53-54**, 415 (1987).
- ¹⁷S. Abe and Y. Toyozawa, *J. Phys. Soc. Jpn.* **50**, 2185 (1981).
- ¹⁸J. Ihm and J. C. Phillips, *Phys. Rev. B* **27**, 7803 (1983).
- ¹⁹J. Ihm, *J. Phys. C* **18**, 4741 (1985).
- ²⁰G. D. Cody, T. Tiedje, B. Abeles, B. Brooks, and Y. Goldstein, *Phys. Rev. Lett.* **47**, 1480 (1981).
- ²¹C. T. Chan, Steven G. Louie, and J. C. Phillips, *Phys. Rev. B* **35**, 2744 (1987).
- ²²A. Ksendov, F. K. Pollak, G. P. Espinosa, and J. C. Phillips, *Phys. Rev. B* **35**, 2740 (1987).